2021 60th IEEE Conference on Decision and Control (CDC)
December 13-15, 2021. Austin, Texas

Fuel-optimal program for atmospheric vertical powered landing

Hubert Ménou and Eric Bourgeois and Nicolas Petit

2021 60th IEEE Conference on Decision and Control (CDC) | 978-1-6654-3659-5/21/$31.00 ©2021 IEEE | DOI: 10.1109/CDC45484.2021.9682902

***Abstract*— This paper studies the problem of vertical powered landing through a non-negligible density atmosphere. Several constraints are considered, one of them prevents hovering flight. The findings of the paper extend the results from the literature on atmosphere-free problems. The main contribution establishes the nature of the fuel-optimal control sequence. Sufficient and necessary conditions are provided that guarantee the Min-Max nature of the normal extremals. Abnormal extremals are also shown to be either Min or Max.**

I. INTRODUCTION

Powered landing is a critical problem for reusable launchers and planetary exploration. In these contexts, minimizing the fuel consumption is a very natural and desirable objective, which can be directly transcripted as a free-final-time optimal control problem under constraints. Such problems, for which abundant literature is available, have been formulated very early in the development of space exploration programs.

Historically, Meditch [1] and then Shi & Eckstein [2] have offered analytic solutions for the (atmosphere-free) vertical Moon landing problem. Since then, due to the spectacular development of reusable launcher technologies, powered landing strategies have been successfully addressed using numerical methods [3]–[8]. Due to the non-negligible effects of the atmosphere, the analytical results derived for the Moon landing problem can not be directly adapted to the problem of Earth landing. Yet, analytical results on this problem would still represent valuable assets. On the one hand, analytic solutions are very useful to assess the quality of the numerical methods, by providing well-described reference solutions to standardized problems, see *e.g.* [9]–[13]. Further, when analytical investigations establish the switching structure of the solution, very efficient numerical methods can be employed, using a reduced number of unknown variables [11], [12], [14]. For complex dynamics and high-dimensional systems, obtaining such analytical results is usually considered as out-of-reach [15]. It is thus of importance to select only dominant factors while leaving out unnecessary details in the modeling. Following this modus operandi, we consider a simplified (but not simplistic) representation of the general powered landing problem and establish a non-trivial result.

This paper considers one key element: the effects of atmosphere. The model under study builds upon the variable-mass model of a spacecraft (here referred to as a rocket) considered in [1] and incorporates atmospheric effects in the form of an altitude-dependent bias of the thrust. In this model of the final phase of the powered landing, the thrust generator is always turned on and the thrust is upper and lower-bounded in a way that prevents hovering flight.

Intuitively, one could expect that it is more efficient to wait until the last feasible moment to use maximal thrust, as early efforts trying to slow down the rocket are likely to be less effective due to the varying mass scaling of the dynamics. The contribution of this paper is to establish conditions under which fuel-optimal vertical powered landing through the atmosphere is indeed of this expected Min-Max nature.

The arguments of proof are as follows. Under simple assumptions on the atmosphere pressure model (decrease, convexity), the optimal thrust program is first shown to have a max-min-max structure, based on the Pontryagin's Maximum Principle (PMP). Compared to [1], some sharper differential inequalities on the adjoint states are necessary to conclude. Also, both normal and abnormal extremals need to be tackled. Then, using additional inequality constraints derived from the Implicit Function Theorem (IFT), min-max structures are proven to be more fuel-optimal than max-min-max structures. These conditions can be checked numerically, over a finite domain. It is also shown that these conditions hold for zero atmosphere (and scarce atmosphere, using a continuity argument), which makes a connection with [1].

The paper is organized as follows. In Section II, the dynamics and the powered landing problem are presented. In Section III, the flight envelope is described based on flow analysis and differential inequalities. In Section IV, the optimal thrust program is shown to be min-max using the PMP and the IFT. Finally, we provide numerical details in Section V, and concluding remarks in Section VI.

II. PROBLEM STATEMENT

A. A Rocket Model

The rocket is modeled as an axially symmetrical rigid body, moving vertically, with altitude h, speed v and total mass m, subjected to its weight in a constant

H. Ménou (hubert.menou@mines-paristech.fr) and N. Petit (nicolas.petit@mines-paristech.fr) are with Centre Automatique et Systèmes (CAS), MINES ParisTech, Université PSL, 75006 Paris, France, and E. Bourgeois (eric.bourgeois@cnes.fr) is with CNES, Direction des lanceurs, 52, rue Jacques Hillairet, 75612 Paris Cedex, France.

This work was partially supported by CNES.

Authorized licensed use limited to: ECOLE DES MINES PARIS. Downloaded on February 10,2022 at 09:24:16 UTC from IEEE Xplore. Restrictions apply.

gravity field g, and its engine thrust T. The dynamics write $\dot{h} = v, \quad \dot{v} = -g + \frac{T(h,Q)}{m}, \quad \dot{m} = -Q$ where Q is the engine flow. Negative speed conveys descending movement. The thrust is defined as follows

$$T(h, Q) = g\, \mathrm{I_{SP}}\, Q - S\, P(h) \tag{1}$$

where $\mathrm{I_{SP}}$ is the engine specific impulse, S is the rocket section area and P is the atmospheric pressure. During the powered landing, the rocket engine is always firing and Q satisfies

$$0 < \underline{Q} \leq Q \leq \overline{Q} \tag{2}$$

The thrust model used in (1) conveys the net contribution of the actual thrust, taking into account the aerodynamic effects via an altitude dependent bias. Because the engine is firing, as pictured in Figure 1, the sole effect of the atmosphere is through the atmospheric pressure in (1). This is a valid approximation when the movement is vertical, but would not be directly applicable for planar or 3D movements as the aerodynamic drag model and its interaction with the engine thrust could be more complex in the wake of the thrust flame.

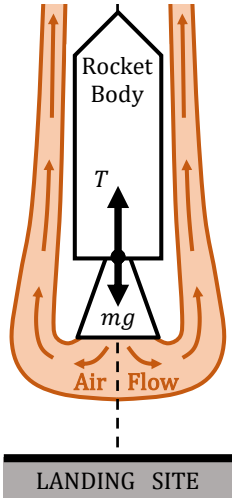

Fig. 1. Powered descent for vertical landing.

In the problem setup under consideration, the constraints (2) are s.t. the net thrust is always positive, *i.e.* $\underline{Q}$ is s.t.

$$g\, \mathrm{I_{SP}}\, \underline{Q} - S \max_{h \geq 0} P(h) > 0. \tag{3}$$

Normalized dynamics: The following normalized variables are introduced

$$u \triangleq 2\frac{Q-\underline{Q}}{\overline{Q}-\underline{Q}} - 1, \quad u \in [-1, 1],$$
$$y_1 \triangleq \frac{h}{g\, \mathrm{I_{SP}}}, \quad y_2 \triangleq \frac{v}{g\, \mathrm{I_{SP}}}, \quad y_3 \triangleq \frac{2m}{\overline{Q}-\underline{Q}}, \quad y \triangleq (y_1, y_2, y_3)^\top,$$
$$\kappa \triangleq \frac{1}{\mathrm{I_{SP}}}, \quad r \triangleq \frac{\overline{Q}+\underline{Q}}{\overline{Q}-\underline{Q}}, \quad \pi(y_1) \triangleq P(g\, \mathrm{I_{SP}}\, y_1)\frac{2S}{g\, \mathrm{I_{SP}}\, (\overline{Q}-\underline{Q})}\ .$$

This yields the control-affine dynamics in $\mathbb{R}^3$

$$\dot{y} = f(y) + ug(y), \tag{4}$$

$$\text{(Altitude)} \qquad \dot{y}_1 = y_2 \tag{5}$$

$$\text{(Speed)} \qquad \dot{y}_2 = \frac{r + u - \pi(y_1)}{y_3} - \kappa \tag{6}$$

$$\text{(Mass)} \qquad \dot{y}_3 = -(r + u). \tag{7}$$

B. Specificities

The system under study in this paper is described by the two following assumptions. *Assumption 1: (Pressure model properties)* The normalized pressure function π, is of class C^2, and $\pi > 0$, $\pi' < 0$, $\pi'' > 0$.
This assumption is very general and holds for all reference Earth atmosphere models, such as [16].

The fuel tank being finite, there are two positive bounds $\underline{y}_3$ and $\bar{y}_3$ s.t. $\underline{y}_3 \leq y_3 \leq \bar{y}_3$.

The engine flow is bounded s.t. in the least favorable mass and altitude scenario, the net thrust strictly compensates the gravity. Denote $\underline{a_{cc}} \triangleq \frac{r-1-\pi(0)}{y_3^+} - \kappa$. For any altitude, any speed, and any mass lower than $\bar{y}_3$, a *positive acceleration* is assumed, as stated below. *Assumption 2: (Thrust dominance)* $\dot{y}_2 \geq \underline{a_{cc}} > 0$.
Assumption 2 implies condition (3), shows that $r > 1$ and prevents hovering. Reaching null speed at a positive altitude is thus an undesired behavior and is not a steady state.

C. Optimal Control Problems

A natural goal sought for rocket landing is to maximize the final mass [1], or equivalently to minimize the fuel consumption, as it is a critical variable to deal with uncertainties during the flight. Landing is defined as final null altitude and (vertical) velocity. A constrained optimal control problem in free final time depending on an initial state y^0 can then be formulated.

Problem 1: (Fuel optimal landing with state inequality path constraints)

$$\begin{aligned} \min_{u(.),\, t_f} \quad & \int_0^{t_f} r + u(s)ds \\ \text{s.t.} \quad & \dot{y} = f(y) + ug(y), \ \ |u| \leq 1, \\ & y(0) = y^0, y_1(t_f) = y_2(t_f) = 0, \\ & y_1(t) \geq 0, \ y_2(t) \leq 0, \ y_3(t) \in [\underline{y}_3, \bar{y}_3] \end{aligned} \tag{8}$$

State constraints (8) are meant for any t in $[0, t_f]$. Additionally, we will consider another formulation where the state constraints (8) have been removed, as they will be shown to be automatically satisfied.

Problem 2: (Fuel optimal landing)

$$\begin{aligned} \min_{u(.),\, t_f} \quad & \int_0^{t_f} r + u(s)ds \\ \text{s.t.} \quad & \dot{y} = f(y) + ug(y), \ \ |u| \leq 1, \\ & y(0) = y^0, y_1(t_f) = y_2(t_f) = 0 \end{aligned}$$

Studying Problem 2 will help us describe the solutions of Problem 1.

D. Notations

The sign function is $\mathrm{Sgn}\,(a) = +1$ if $a > 0$, $\mathrm{Sgn}\,(a) = -1$ if $a < 0$ and $\mathrm{Sgn}\,(0) = 0$. For $F : X \subset \mathbb{R}^n \to \mathbb{R}^n$ a smooth vector field, its flow is denoted by $\phi_F : \mathbb{R}^+ \times \mathbb{R}^n \to \mathbb{R}^n$. Maximal solutions of an ordinary differential equation are solutions that cannot be extended in time. Comparisons between vectors must be understood element-wise.

Authorized licensed use limited to: ECOLE DES MINES PARIS. Downloaded on February 10,2022 at 09:24:16 UTC from IEEE Xplore. Restrictions apply.

III. Premilinaries on the dynamics

This section aims at describing conditions under which state path inequalities (8) can be ignored. A detailed study of the dynamics is conducted. First, the altitude and speed dynamics are studied using surfaces of $\mathbb{R}^3$ s.t. any trajectory that *lands* must start between these surfaces. This region is called the *flight envelop*. Then, the mass constraint is discussed.

Let us denote the domain $\mathcal{D} \triangleq \mathbb{R}^+ \times \mathbb{R}^- \times (0, \bar{y}_3]$. Below, we say that a trajectory starting at some $y^0 \in \mathcal{D}$ *lands* applying the thrust $u(.)$ if it reaches $y_1(t_f) = y_2(t_f) = 0$ for some $t_f > 0$. Note that the minimum mass constraint is not included in this first part of the discussion.

Beforehand, remark that there is a unique time T_u associated to a control $u(.)$ s.t.

$$y_3^0 - \int_0^{T_u} r + u(s)ds = 0. \tag{9}$$

Since $r + u \geq r - 1 > 0$, the map $t \to 1/y_3(t)$ is not integrable near T_u because of (7). Thus, the maximal solution of (4) starting at $y^0 \in \mathcal{D}$ is defined on the interval $[0, T_u)$. If $u \equiv \sigma$ is constant, then $T_\sigma = y_3^0/(r+\sigma)$.

Lemma 1: Let $\sigma \in [-1, 1]$ a constant parameter. For any y_2^0 and y_3^0, there is a unique $y_1^0(\sigma, y_2^0, y_3^0)$ s.t. a trajectory starting at $(y_1^0(\sigma, y_2^0, y_3^0), y_2^0, y_3^0)^\top \in \mathcal{D}$ lands when applying the constant thrust $u \equiv \sigma$.

Proof: The maximal solution y of (4) with $u \equiv \sigma$, starting at $y^0 \in \mathcal{D}$, is defined on $[0, T_\sigma)$. $y_2(.)$ is continuous, increasing and diverges to $+\infty$ as t tends to T_σ. Thus, there is a unique time, denoted $t_*(y_1^0) \in [0, T_\sigma)$ s.t. $y_2(t_*(y_1^0)) = 0$. The IFT applied with Assumption 2, on equation[1]

$$\phi_{f+\sigma g}\left(t_*(y_1^0), (y_1^0, y_2^0, y_3^0)^\top\right)\big|_2 = 0 \tag{10}$$

shows that the application that maps y_1^0 into t_* is actually continuous, and differentiable, for all $y_1^0 \geq 0$. Then, define:

$$\eta : \mathbb{R}^+ \ni z \mapsto \phi_{f+\sigma g}(t_*(z), (z, y_2^0, y_3^0)^\top)\big|_1 \in \mathbb{R}. \tag{11}$$

From the regularity of $f + \sigma g$, the flow $\phi_{f+\sigma g}$ is continuous and thus η is continuous. Necessarily, $\eta(0) < 0$. Moreover, since the acceleration is lower-bounded by $\underline{a_{cc}}$, it is possible to find an altitude $y_1^{crit} > 0$ large enough s.t. $\eta(y_1^{crit}) > 0$. Therefore, there is a $y_1^* \geq 0$ s.t. $\eta(y_1^*) = 0$. Using $t_f = t_*(y_1^*)$, one has $y_1(t_f) = y_2(t_f) = 0$ by construction of η. A comparison argument, as in the proof of Proposition 1, shows that η is actually increasing, proving the uniqueness of y_1^*. It yields $y_1^* = y_1^0(\sigma, y_2^0, y_3^0)$ using the above-mentioned variables. ∎

Let us denote $\Sigma_{\max}$ (respectively $\Sigma_{\min}$) the set of initial conditions s.t. landing is successful, at mass $y_3^f \in (0, \bar{y}_3]$, when applying a constant maximum (resp. minimum) thrust. Denoting $y_1^{\max}(y_2, y_3) \triangleq y_1^0(1, y_2, y_3)$ and $y_1^{\min}(y_2, y_3) \triangleq y_1^0(-1, y_2, y_3)$, it yields

$$\Sigma_{\max} \triangleq \{(y_1^{\max}(y_2, y_3), y_2, y_3) : y_2 \leq 0, y_3 \in (0, \bar{y}_3]\},$$
$$\Sigma_{\min} \triangleq \{(y_1^{\min}(y_2, y_3), y_2, y_3) : y_2 \leq 0, y_3 \in (0, \bar{y}_3]\}.$$

Moreover, using flows of the backward-time dynamics, for $\sigma \in [-1, 1]$, define

$$\Sigma_\sigma \triangleq \left\{\phi_{-(f+\sigma g)}\left(t, (0, 0, y_3^f)^\top\right) : 0 \leq t \leq \frac{\bar{y}_3 - y_3^f}{r + \sigma}, \; 0 < y_3^f \leq \bar{y}_3\right\}$$

which provides the relations $\Sigma_{\max} = \Sigma_1$ and $\Sigma_{\min} = \Sigma_{-1}$. It is noteworthy that $y_1^{\max}(y_2, y_3) \leq y_1^{\min}(y_2, y_3)$, implying that $\Sigma_{\max}$ is always "below" $\Sigma_{\min}$, as pictured in Figure 3.

Note that the applications $y_1^{\min}$ and $y_1^{\max}$ are continuous: this property comes from the continuity of the flows and the formal definition of Σ_σ. Continuity can also be proven using the IFT on function η from equation (11), considering y_2^0 and y_3^0 as variables.

Proposition 1: For any $y^0 \in \mathcal{D}$, if $y_1^{\min}(y_2^0, y_3^0) < y_1^0$ then for any control $u(.)$ in $[-1, 1]$ the dynamics reaches null speed at a positive altitude.

Proof: Consider $y^0 \in \mathcal{D}$ s.t. $y_1^{\min}(y_2^0, y_3^0) < y_1^0$ and denote $\tilde{y}^0 \triangleq (y_1^{\min}(y_2^0, y_3^0), y_2^0, y_3^0)^\top$. Let $\tilde{y}$ be the maximal solution of (4) with $u \equiv 1$ and y be the maximal solution of (4) for some measurable function u satisfying $|u| \leq 1$ at all times. y starts at y^0 and $\tilde{y}$ at $\tilde{y}^0$. They are respectively defined on $[0, T_1)$ and $[0, T_u)$, where $T_u \leq T_1$. Using mass as a time-varying scaling, we get

$$\begin{pmatrix}\dot{y}_1(t)\\ \dot{y}_2(t)\end{pmatrix} \geq K\left(t, \begin{pmatrix}y_1(t)\\ y_2(t)\end{pmatrix}\right) \triangleq \begin{pmatrix}y_2(t)\\ -\kappa + \frac{r-1-\pi(y_1(t))}{y_3^0 - t(r-1)}\end{pmatrix}$$

for any $t \in [0, T_u)$. By construction, $\tilde{y}$ satisfies the equality version of this equation. Thus, comparison Lemma 5 (in Section VII) yields

$$\tilde{y}_1(t) \leq y_1(t), \quad \tilde{y}_2(t) \leq y_2(t), \quad \forall t \in [0, T_u).$$

Since y_2 is continuous, increasing and diverges as $t \to T_u$, there is a unique $t_* \in [0, T_u)$ s.t. $y_2(t_*) = 0$. Therefore, $y_1(t_*) \geq \tilde{y}_1(t_*) \geq 0$. Using a Taylor expansion on (5) with the initial conditions shows that the last inequality is strict, whence the proposition. ∎

Using a very similar proof, one shows the following result.

Proposition 2: For any $y^0 \in \mathcal{D}$, if $y_1^{\max}(y_2^0, y_3^0) > y_1^0$ then for any control $u(.)$ in $[-1, 1]$ the dynamics reaches null altitude at a negative speed.

Proposition 1 defines the notion of being *too high*, meaning that if the rocket starts its powered descent above $\Sigma_{\min}$ (in terms of altitude), then it will either lack fuel before reaching null speed, or go back up before touching the ground and then lack fuel at a non-zero altitude. In both cases, landing fails. Proposition 2 is the exact equivalent for the notion of being *too low*, meaning that the rocket will hit the ground at a non-zero speed if it starts below $\Sigma_{\max}$.

[1]Here $\star|_i$ denotes the i^{th} component of $\star$.

Authorized licensed use limited to: ECOLE DES MINES PARIS. Downloaded on February 10,2022 at 09:24:16 UTC from IEEE Xplore. Restrictions apply.

Further, note that if a trajectory lands, s.t. the mass remains in $[\underline{y}_3, \bar{y}_3]$, then the acceleration is upper bounded by $\bar{a}_{cc} \triangleq -\kappa + \frac{r+1}{\underline{y}_3}$ for any positive time. Since the fuel flow is lower-bounded, the mass can remain in $[\underline{y}_3, \bar{y}_3]$ for at most $T_{\max} \triangleq \frac{\bar{y}_3 - \underline{y}_3}{r-1}$ Therefore, for any positive time, the speeds are lower-bounded by $\underline{y}_2$ and the altitudes are upper-bounded by $\bar{y}_1$ s.t.

$$\underline{y}_2 \triangleq -\bar{a}_{cc} T_{\max} \quad \text{and} \quad \bar{y}_1 \triangleq \bar{a}_{cc} \frac{T_{\max}^2}{2}. \tag{12}$$

Let us define by $\mathcal{F} \subset \mathcal{D}$ the *flight envelop*, as the set of states y lying between $\Sigma_{\max}$ and $\Sigma_{\min}$ (in terms of altitude), and satisfying

$$y_1 \leq \bar{y}_1, \quad y_2 \geq \underline{y}_2, \quad \text{and} \quad \underline{y}_3 \leq y_3 \leq \bar{y}_3. \tag{13}$$

Consequently, if $y^0 \in \mathcal{F}$ and Problem 2 has a solution, then altitude and speed constraints are enforced. If $y^0 \in \mathcal{D} \backslash \mathcal{F}$, then Problems 1 and 2 cannot have solutions.

Leaving out the limit cases of $\Sigma_{\max}$ and $\Sigma_{\min}$, for which landing can be achieved by applying respectively the maximum and the minimum thrust, for the whole duration of the flight, we introduce

$$\mathcal{F}^* \triangleq \mathcal{F} \backslash (\Sigma_{\max} \cup \Sigma_{\min}). \tag{14}$$

The following result discusses feasibility of the landing. Optimality will be studied later on in Section IV.

Proposition 3: If y^0 belongs to $\mathcal{F}^*$, then there is always a control u of structure min-max that lands.

Proof: The min-max structure denotes a 2 step sequence starting with minimum value of the control and ending with maximum value. For such y^0, denote $\tilde{y}^0 \triangleq (y_1^{\min}(y_2^0, y_3^0), y_2^0, y_3^0) \in \Sigma_{\min}$. Since $y^0 \in \mathcal{F}^*$, then $y_1^{\max}(y_2^0, y_3^0) < y_1^0 < y_1^{\min}(y_2^0, y_3^0)$.

Let us denote y and $\tilde{y}$ the maximal solutions of equation (4) with $u \equiv -1$, starting respectively at y^0 and $\tilde{y}^0$. Then, using similar comparisons as in the previous proof, $y_1(t) < \tilde{y}_1(t)$ and $y_2(t) < \tilde{y}_2(t)$ for all positive times. Thus, one deduces that y_1 reaches zero at some time $t' > 0$, before y_2 does. Moreover, the map

$$\xi : t \in [0, t'] \to y_1(t) - y_1^{\max}(y_2(t), y_3(t)) \in \mathbb{R} \tag{15}$$

is continuous, and satisfies $\xi(0) > 0$ since the trajectory starts strictly above $\Sigma_{\max}$, and $\xi(t') < 0$ since $(0, y_2(t'), y_3(t'))$ is necessarily below $\Sigma_{\max}$ in terms of altitude (recall that $y_2(t') < 0$). Thus, there is a time $t'' \leq t'$ s.t. $y(t'') \in \Sigma_{\max}$. The desired min-max control law equals -1 on $[0, t'')$ and $+1$ for times $t \geq t''$. ∎

As far as the mass is concerned, since it is a continuous decreasing function of time, enforcing the terminal constraint $y_3(t_f) \geq \underline{y}_3$ is sufficient to guarantee mass constraint (8).

Therefore, *only the simplified Problem 2 needs to be solved*. If there is a solution that satisfy $y_3(t_f) \geq \underline{y}_3$, then Problem 1 shares the same solution. Otherwise, if $y_3(t_f) < \underline{y}_3$, then Problem 1 has no solutions. Indeed, since the solution is fuel-optimal, there is no other way to land with a greater final mass.

IV. OPTIMAL THRUST PROGRAMS

This section focuses exclusively on Problem 2, which, according to the previous discussion gives an answer to Problem 1 or proves its infeasibility. We aim at proving that optimal controls are of min-max nature, where one of the Min or Max arcs may be absent. To establish this result (Theorem 1), we proceed as follows. First, stationary conditions are derived from the PMP. Then, using properties of the second adjoint state variable, the optimal thrust program is shown to be max-min-max. Finally, the first maximum arc is shown to be absent under one (mild) additional assumption on the atmosphere model (Assumption 4).

A. Fuel Optimal Landing

Consider $y^0 \in \mathcal{F}$. Let u be an optimal thrust program for Problem 2 and y be the corresponding trajectory. Let t_f be the time-of-flight. It is assumed that $y_3(t_f) \geq \underline{y}_3$. Thus, from the previous section, y lies in $\mathcal{F}$.

The Hamiltonian of Problem 2 is defined as

$$H \triangleq \lambda_0(r + u) + \lambda^\top (f(y) + u g(y)) \tag{16}$$

where $\lambda_0 \in \mathbb{R}$ and $\lambda : [0, t_f] \to \mathbb{R}^3$ denote the adjoint states. To study the control-affine Hamiltonian, consider the switching function

$$\Gamma(t) \triangleq \lambda_0 + \lambda(t)^\top g(y(t)) = \lambda_0 + \frac{\lambda_2(t)}{y_3(t)} - \lambda_3(t). \tag{17}$$

The Pontryagin maximum principle (PMP), as stated in [15, Thm. 2.2.1], yields

$$(\lambda_0, \lambda(t)) \neq 0_{\mathbb{R}^4}, \quad \forall t \in [0, t_f] \tag{18}$$

$$\dot{\lambda}_1 = \lambda_2 \frac{\pi'(y_1)}{y_3} \tag{19}$$

$$\dot{\lambda}_2 = -\lambda_1 \tag{20}$$

$$\dot{\lambda}_3 = \frac{\lambda_2}{y_3^2}(r + u - \pi(y_1)) \tag{21}$$

$$u = -\operatorname{Sgn}(\Gamma(t)), \quad \text{when } \Gamma(t) \neq 0 \tag{22}$$

$$\lambda(t_f) = \begin{pmatrix} \nu_1 & \nu_2 & 0 \end{pmatrix}^\top, \quad (\nu_1, \nu_2) \in \mathbb{R}^2 \tag{23}$$

Equation (18) states the non-triviality of the adjoint states. Since the integral cost, the dynamics and the endpoint constraints are time-invariant, the Hamiltonian is constant along the extremals and for such a free time, fixed endpoint problem, this constant is zero [17], [18, Thm. 7.8.1]

$$H(t) \equiv 0, \quad \forall t \in [0, t_f]. \tag{24}$$

The optimal pairs (y, u) are called *abnormal* extremals [19], [20] if $\lambda_0 = 0$, and *normal* extremals if $\lambda_0 \neq 0$. We now proceed to establish some intermediate results on the adjoint states.

Proposition 4: $(\lambda_1(t), \lambda_2(t)) \neq (0, 0)$ for all $t \in [0, t_f]$.

Proof: The linear time-varying dynamics of (λ_1, λ_2) is Lipschitz in (λ_1, λ_2) and continuous in time. Therefore, from the Cauchy-Lipschitz theorem, any maximal solution is unique. Thus, if there is a t_0 s.t. $(\lambda_1, \lambda_2)(t_0) = 0$,

Authorized licensed use limited to: ECOLE DES MINES PARIS. Downloaded on February 10,2022 at 09:24:16 UTC from IEEE Xplore. Restrictions apply.

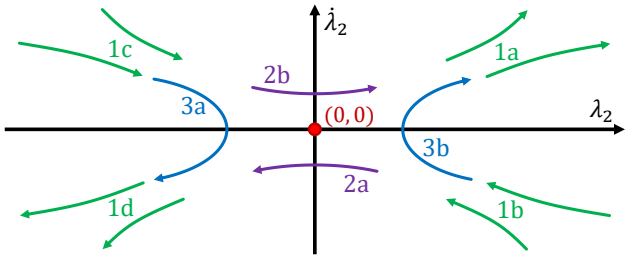

Fig. 2. Possible scenarios for $(\lambda_2, \dot\lambda_2)$. The origin is prohibited due to Proposition 4.

then $\lambda_2 \equiv 0$ over $[0, t_f]$, implying $\lambda_3 \equiv 0$ from (21) and (23) and then $\lambda_0 = 0$ from (24), violating (18). ■

Now, remark that the sign of λ_2 and $\dot\lambda_2$ can be extrapolated from the following second-order equation

$$\ddot\lambda_2 = a(t)\lambda_2, \text{ where } a(t) \triangleq -\frac{\pi'(y_1(t))}{y_3(t)} > 0. \tag{25}$$

Indeed, the cones $\mathbb{R}^+ \times \mathbb{R}^+$ and $\mathbb{R}^- \times \mathbb{R}^-$ are invariant through the dynamics (25). This shows that if λ_2 or $\dot\lambda_2$ is null at some $t_\lambda \in (0, t_f)$, then they will both remain in one of these cones after t_λ. Further, from Proposition 4 and (25), they will actually remain in interior subsets of these cones for times $t > t_\lambda$. Hence, by an exhaustive enumeration of possible cases we can state the following result.

Proposition 5: $(\lambda_2, \dot\lambda_2)$ necessarily match one of these conditions, as illustrated in Figure 2:

1) λ_2 and $\dot\lambda_2$ are never zero on $(0, t_f)$:
   a) $\lambda_2 > 0$ and $\dot\lambda_2 > 0$ on $(0, t_f)$,
   b) $\lambda_2 > 0$ and $\dot\lambda_2 < 0$ on $(0, t_f)$,
   c) $\lambda_2 < 0$ and $\dot\lambda_2 > 0$ on $(0, t_f)$,
   d) $\lambda_2 < 0$ and $\dot\lambda_2 < 0$ on $(0, t_f)$,
2) $\exists! t_\lambda \in (0, t_f) : \lambda_2(t_\lambda) = 0$ and $\dot\lambda_2 \neq 0$ on $[0, t_f]$:
   a) $\text{Sgn}(\lambda_2(t)) = -\text{Sgn}(t - t_\lambda)$ and $\dot\lambda_2 < 0$,
   b) $\text{Sgn}(\lambda_2(t)) = \text{Sgn}(t - t_\lambda)$ and $\dot\lambda_2 > 0$,
3) $\exists! t_\lambda \in (0, t_f) : \dot\lambda_2(t_\lambda) = 0$ and $\lambda_2 \neq 0$ on $[0, t_f]$:
   a) $\text{Sgn}\left(\dot\lambda_2(t)\right) = -\text{Sgn}(t - t_\lambda)$ and $\lambda_2 < 0$,
   b) $\text{Sgn}\left(\dot\lambda_2(t)\right) = \text{Sgn}(t - t_\lambda)$ and $\lambda_2 > 0$.

Note that for scenarios 1a and 1d (resp. scenarios 1b and 1c), either λ_2 or $\dot\lambda_2$ can be zero at $t = 0$ (resp. at $t = t_f$). Also, note that for scenario 2, λ_2 is necessarily non-zero at $t = 0$ and $t = t_f$ since $\dot\lambda_2$ is of constant sign. The same kind of remark applies to scenario 3 as well. The goal is to state whether these scenarios are consistent with conditions (18)-(23), and if so to what control structure they refer to.

Proposition 6: Abnormal extremals are optimal programs of constant thrust.

Proof: For abnormal extremals, $\lambda_0 = 0$. Using equation (24) at $t = t_f$ yields $\nu_2 = 0 = \lambda_2(t_f)$. Thus, from Proposition 5, λ_2 has a constant non-zero sign over $[0, t_f)$. Moreover, from (21) and (23), one has

$$\text{Sgn}(\lambda_3(t)) = -\text{Sgn}(\lambda_2(t)), \quad \forall t \in [0, t_f). \tag{26}$$

Therefore, for any $t \in [0, t_f)$: $\text{Sgn}(\Gamma(t)) = \text{Sgn}(\lambda_2)$. Hence, u has a constant value in $\{-1, +1\}$ over $[0, t_f)$. ■

This latest proposition shows that abnormal extremals require the initial state y^0 to be on constant thrust trajectories achieving landing, *i.e* $y^0 \in \Sigma_{\max}$ or $y^0 \in \Sigma_{\min}$ must hold for these extremals.

From now on, we consider normal extremals only and without loss of generality[2], we consider $\lambda_0 = 1$. Let us define

$$b(t) \triangleq \frac{\pi(y_1(t))}{y_3(t)}$$

Note that from Assumption 1 and the sign of y_2, one can show that $a(.)$ and $b(.)$ are increasing from a study of their derivatives. Also, for all times in $[0, t_f]$, a and b are respectively lower and upper-bounded by

$$\underline{a} \triangleq -\frac{\pi'(\bar y_1)}{\bar y_3} \text{ and } \bar b \triangleq \frac{\pi(0)}{\underline{y}_3}. \tag{27}$$

Let us define $\gamma(t) \triangleq \dot\lambda_2(t) + \lambda_2(t) b(t)$, which satisfies:

$$\frac{d\Gamma}{dt}(t) = \Gamma'(t) = \frac{\gamma(t)}{y_3(t)} \tag{28}$$

Since y_3 is positive, γ carries the sign of Γ'. From this point, Γ is the subject of our investigations.

Lemma 2: If $\gamma < 0$ over $(0, t_f)$, then Γ is null at most on a singular $t \in [0, t_f]$.

Lemma 3: $\Gamma < 0$ in the neighborhood of t_f.

Proof: Eq. (24) at t_f yields $\nu_2 = -(r + u(t_f))/\dot y_2(t_f)$. Thus, one gets $\Gamma(t_f) = -\frac{\kappa y_3(t_f) + \pi(0)}{y_3(t_f)\dot y_2(t_f)} < 0$. The conclusion follows from the continuity of $\Gamma(.)$. ■

λ_2 must be non-positive in a neighborhood of t_f. Indeed, let us assume that there is a time t' s.t. λ_2 is positive on $[t', t_f)$. Note that $\lambda_2(t_f)$ may be null. Then, using (21) and (23), λ_3 would necessarily be negative on $[t', t_f)$, leading to $\Gamma(t) > 0$ for t in $[t', t_f]$, which contradicts Lemma 3. It eliminates scenarios 1a, 1b, 2b and 3b.

Moreover, note that scenario 1d necessarily corresponds to min-max programs, where one arc may be absent, for it satisfies Lemma 2.

Then, the three remaining scenarios, namely 1c, 2a and 3a, require a refined sign study of λ_2 and $\dot\lambda_2$. Using differential equations bounding λ_2, we can establish bounds on γ tight enough to derive valuable sign information.

Definition 1: For a constant $c > 0$ and $t_0 \in (0, t_f)$, the C^2 function: $x_c : [0, t_f] \to \mathbb{R}$ is defined as the unique solution of the initial value problem $\ddot x_c = c x_c$ with $x_c(t_0) = \lambda_2(t_0)$ and $\dot x_c(t_0) = \dot\lambda_2(t_0)$, or

$$x_c(t) = \lambda_2(t_0)\cosh\sqrt{c}(t - t_0) + \frac{\dot\lambda_2(t_0)}{\sqrt{c}}\sinh\sqrt{c}(t - t_0).$$

Inspired from the definition of γ above, let us denote

$$\gamma_c(t) \triangleq \dot x_c(t) + x_c(t) b(t). \tag{29}$$

and introduce $z_\lambda \triangleq (\lambda_2, \dot\lambda_2)^\top$ and $\underline{z} \triangleq (x_{\underline{a}}, \dot x_{\underline{a}})^\top$ s.t.

$$\dot z_\lambda = F(t, z_\lambda) \triangleq \begin{pmatrix} 0 & 1 \\ a(t) & 0 \end{pmatrix} z_\lambda. \tag{30}$$

[2]Equations being linear in λ, one can consider λ/λ_0 instead of λ.

Authorized licensed use limited to: ECOLE DES MINES PARIS. Downloaded on February 10,2022 at 09:24:16 UTC from IEEE Xplore. Restrictions apply.

The next proofs require the following assumption.

Assumption 3: The constants in (27) are s.t. $\bar{b} < \sqrt{\underline{a}}$.

Proposition 7: For scenario 2a, $\gamma(t) < 0, \forall t \in [0, t_f]$.

Proof: Here, $\dot{\lambda}_2 < 0$ and $\mathrm{Sgn}\,(\lambda_2(.)) = -\mathrm{Sgn}\,(. - t_\lambda)$, where $t_\lambda \in (0, t_f)$. In this proof only, we consider the functions from Definition 1 with $t_0 = t_\lambda$. It leads to

$$\gamma_{\underline{a}}(t) = \dot{\lambda}_2(t_\lambda)\left(\cosh\sqrt{\underline{a}}(t-t_\lambda) + \frac{b(t)}{\sqrt{\underline{a}}}\sinh\sqrt{\underline{a}}(t-t_\lambda)\right)$$

For any $t > t_\lambda$, $\gamma_{\underline{a}}(t) < 0$. Since a increases, scenario 2a yield $z_\lambda(t_\lambda) = z_{\underline{a}}(t_\lambda)$ and for any $t \in [t_\lambda, t_f]$

$$\dot{z}_\lambda(t) = F(t, z_\lambda(t)) \text{ and } \dot{z}_{\underline{a}}(t) \leq F(t, z_{\underline{a}}(t)). \tag{31}$$

Comparison Lemma 5 yields $z_\lambda(t) \leq z_{\underline{a}}(t)$ on $[t_\lambda, t_f]$. As a consequence

$$\gamma(t) \leq \gamma_{\underline{a}}(t) < 0, \quad \forall t \in [t_\lambda, t_f]. \tag{32}$$

For any $t < t_\lambda$, $\gamma_{\underline{a}}(t) < 0$ when Assumption 3 is satisfied. The same reasoning applies, except that $\lambda_2(t) > 0$ this time, and that comparison Lemma 5 has to be applied in backward-time. It shows that $\gamma(t) \leq \gamma_{\underline{a}}(t) < 0$ for any $t \in [0, t_\lambda]$, whence the desired property. ∎

Lemma 3 and Proposition 7 imply that the sign of Γ changes at most once over $[0, t_f]$ for scenario 2a.

Lemma 4: If $\lambda_2 < 0$ over $[0, t_f]$, if $\gamma(t_\gamma) = 0$ for some $t_\gamma \in (0, t_f)$ and if Assumption 3 holds, then: $\gamma(t) < 0, \ \forall t > t_\gamma$.

Proof: By construction $\lambda_2(t_\gamma) = -\dot{\lambda}_2(t_\gamma)/b(t_\gamma)$. Necessarily, $\dot{\lambda}_2(t_\gamma) > 0$. In this proof only, we consider the functions from Definition 1 with $t_0 = t_\gamma$. It yields

$$\gamma_{\underline{a}}(t) = \dot{\lambda}_2(t_\gamma)\Bigg[\left(1 - \frac{b(t)}{b(t_\gamma)}\right)\cosh\sqrt{\underline{a}}(t-t_\gamma) + \frac{b(t)b(t_\gamma) - \underline{a}}{b(t_\gamma)\sqrt{\underline{a}}}\sinh\sqrt{c}(t-t_\gamma)\Bigg] \tag{33}$$

Since b increases, the factor associated to cosh is negative. Also, Assumption 3 yields

$$b(t)b(t_\gamma) - \underline{a} \leq (b(t) + \sqrt{\underline{a}})(b(t) - \sqrt{\underline{a}}) < 0 \tag{34}$$

Thus, $\gamma_{\underline{a}}(t) < 0$ for $t > t_\gamma$. Moreover, $z_\lambda(t_\gamma) = z_{\underline{a}}(t_\gamma)$ holds and since $\lambda_2 < 0$, for any $t \in [t_\gamma, t_f]$:

$$\dot{z}_\lambda(t) = F(t, z_\lambda(t)) \text{ and } \dot{z}_{\underline{a}}(t) \leq F(t, z_{\underline{a}}(t)), \tag{35}$$

The conclusion stems from comparison Lemma 5. ∎

Proposition 8: Under the assumptions of Lemma 4, the sign of Γ changes at most twice on $[0, t_f]$.

Proof: γ can be zero at most on an isolated point. Indeed, γ is continuous and if there is t_0 s.t. $\gamma(t_0) = 0$, then, from Lemma 4, it cannot be zero for greater times. Therefore, from (28), Γ can be zero at most on two isolated points. ∎

Proposition 8 shows that the two remaining scenarios (1c and 3a) corresponds to max-min-max structures. It enables us to state the main result of the subsection.

Proposition 9: Under Assumptions 1, 2 and 3, and for y^0 in $\mathcal{F}$, any solution of Problem 2 is necessarily a max-min-max thrust program, where one or two arcs may be absent.

B. Optimality of Min-Max Programs

We shall now discuss under which conditions min-max trajectories are always more fuel-optimal than max-min-max trajectories, for some $y^0 \in \mathcal{F}^*$.

Let us consider a trajectory y starting at y^0, with thrust structure max-min-max. Denote t_1 its first time of switch (from max to min). The last max arc may be of null duration. Then, for every time $t_1' \in [0, t_1]$, there is a trajectory with thrust structure max-min-max, with first time of switch t_1', that lands, which is guaranteed by applying Proposition 3 at t_1'. Below, we derive conditions under which the trajectory having the smallest first time of switch has the highest final mass, showing that the min-max trajectory starting from y^0 is fuel-optimal.

The second time of switch, denoted t_2, and the final time t_f are implicitly imposed by t_1 so that the rocket lands. This relation will be given later. For the time being, note that the final mass, denoted y_3^f, satisfies

$$\begin{aligned} y_3^0 - y_3^f(t_1) = &(r+1)t_1 + (r-1)(t_2(t_1) - t_1) \\ &+ (r+1)(t_f(t_1) - t_2(t_1)) \end{aligned} \tag{36}$$

The first two components of y are collected in $\mu(y)$, i.e. $\mu(y) \triangleq (y_1, y_2)^\top$. The landing condition is simply: $\mu(y(t_f)) = 0$. Define

$$L(\tau_1, \tau_2, \tau_f) \triangleq \mu\left(\phi_{f+g}(\tau_f - \tau_2, \phi_{f-g}(\tau_2 - \tau_1, \phi_{f+g}(\tau_1, y^0)))\right).$$

Then, the landing condition boils down to

$$L(t_1, t_2, t_f) = 0. \tag{37}$$

It describes the above-mentioned implicit dependence of (t_2, t_f) on t_1. When applicable, the IFT used on (37) provides us with the differentiability and the value of the derivatives of t_2 and t_f with respect to t_1, as

$$\left(\frac{dt_2}{dt_1}, \frac{dt_f}{dt_1}\right)^\top = -\left[\frac{\partial L}{\partial [t_2, t_f]}\right]^{-1} \cdot \frac{\partial L}{\partial t_1} \tag{38}$$

To express these derivatives with respect to t_1, intermediate quantities are introduced. The *transition* matrices $M(t_f)$ and $N(t_2)$ are respectively defined as the unique solutions to the matrix initial value problems

$$\dot{M}(t) = \frac{\partial(f+g)}{\partial y}(y(t)) \cdot M(t) \text{ and } M(t_2) = I_3, \tag{39}$$

$$\dot{N}(t) = \frac{\partial(f-g)}{\partial y}(y(t)) \cdot N(t) \text{ and } N(t_1) = I_3. \tag{40}$$

Let us define R_1, R_2, S_1 and S_2 by

$$\begin{pmatrix} R_1 & R_2 \end{pmatrix}^\top \triangleq \mu\left(M(t_f) \cdot (f-g)(y(t_2))\right) \tag{41}$$

$$\begin{pmatrix} S_1 & S_2 \end{pmatrix}^\top \triangleq \mu\left(M(t_f) \cdot N(t_2) \cdot (f+g)(y(t_1))\right) \tag{42}$$

Since Assumption 2 holds, the invertibility condition of $\frac{\partial L}{\partial [t_2, t_f]}$ needed to apply the IFT boils down to $R_1 \neq 0$.

Authorized licensed use limited to: ECOLE DES MINES PARIS. Downloaded on February 10,2022 at 09:24:16 UTC from IEEE Xplore. Restrictions apply.

Then, one can provide a detailed version of (38)

$$\frac{dt_2}{dt_1} = 1 - \frac{S_1}{R_1} \tag{43}$$

$$\frac{dt_f}{dt_1} = 1 - \frac{1}{\dot{y}_2(t_f)R_1}\left(R_1S_2 - R_2S_1 + S_1\dot{y}_2(t_f)\right) \tag{44}$$

Using the previous terms with equation (36) yields

$$\frac{dy_3^f}{dt_1}(t_1) = \frac{r+1}{\dot{y}_2(t_f)R_1}\Bigg[R_1(S_2 - \dot{y}_2(t_f)) + S_1\left(\dot{y}_2(t_f)\frac{r-1}{r+1} - R_2\right)\Bigg] \tag{45}$$

The conditions that enable us to state that min-max thrust programs are always more fuel-optimal than the max-min-max ones, by allowing us to apply the IFT on L, is thus conveyed by the assumption

Assumption 4: The parameter defined in (41) is s.t. $R_1 \neq 0$, and one has $\frac{dy_3^f}{dt_1}(0) < 0$ for any $y^0 \in \mathcal{F}^*$ s.t. the rocket lands at $y_3(t_f) \geq \underline{y}_3$.

Note that, since it is formulated for any $y^0 \in \mathcal{F}^*$, it is sufficient to check these conditions for $t_1 = 0$ only. Moreover, these conditions can be either checked through (45), analytically - if the pressure model is known well enough and tractable - or numerically.

For illustration purposes only, let us check the validity of Assumption 4 when there is no atmosphere. When $\pi \equiv 0$, every term from (43) and (44) can be explicitly written using the fact that $\frac{r+u}{y_3} = -\frac{\dot{y}_3}{y_3}$ from intermediate integrations, yielding

$$R_1 = \tfrac{2}{r+1}\left(1 - \tfrac{y_3(t_f)}{y_3(t_2)} + \log\tfrac{y_3(t_f)}{y_3(t_2)}\right), \quad R_2 = -\kappa + \tfrac{r-1}{y_3(t_f)}$$
$$S_1 = -\tfrac{2}{r-1}\log\tfrac{y_3(t_2)}{y_3(t_1)}, \qquad\qquad S_2 = -\kappa + \tfrac{r+1}{y_3(t_f)}.$$

R_1 is negative for $y_3(t_2) > y_3(t_f)$. Thus, (45) becomes

$$\frac{dy_3^f}{dt_1}(t_1) = -\frac{4\kappa}{\dot{y}_2(t_f)(r-1)}\frac{1}{R_1}\log\frac{y_3(t_2)}{y_3(t_1)} < 0. \tag{46}$$

The negativity of this quantity gives the desired conclusion. By continuity, the assumption also holds for scarce atmospheres. Further, an example based on a non-scarce tabulated pressure model is treated in Section V.

C. Summary

Under Assumptions 1, 2, 3, and 4, if the final mass y_3^f of the landing min-max trajectory, starting from a y^0 in $\mathcal{F}$, satisfies $y_3^f \geq \underline{y}_3$, then the optimal thrust program of Problem 1 is min-max, where one arc may be absent.

Conversely, if $y_3^f < \underline{y}_3$ or if $y^0 \notin \mathcal{F}$, then Problem 1 has no solution.

Henceforth, it is possible to describe the whole set of feasible initial conditions. Define

$$\Omega(y_3^f) \triangleq \{\phi_{-(f-g)}(\tau_1, \phi_{-(f+g)}(\tau_2, (0,0,y_3^f)^\top)) : \tau_1 \geq 0, \tau_2 \geq 0, (r-1)\tau_1 + (r+1)\tau_2 \leq \bar{y}_3 - y_3^f\}$$

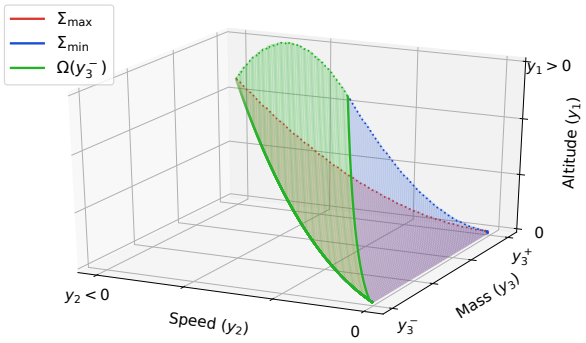

Fig. 3. $\mathcal{F}^{sol}$ is delimited by $\Sigma_{\max}$, $\Sigma_{\min}$, $\Omega(y_3^-)$ and closed by the constraint $y_3 \leq y_3^+$ on the last side. For $\Sigma_{\max}$ and $\Sigma_{\min}$, only the trajectories that land with a mass $y_3(t_f) \geq \underline{y}_3$ are represented. The vertical axis conveys the altitude to ease the visualization.

which denotes the set of states landing at final mass $y_3^f \leq \bar{y}_3$ applying a min-max control. Minimum (resp. maximum) arcs last for τ_1 (resp. τ_2). Thus, the *solution set* $\mathcal{F}^{sol}$ of the initial conditions y^0 s.t. Problem 1 has a solution is

$$\mathcal{F}^{sol} \triangleq \bigcup_{\underline{y}_3 \leq y_3^f \leq \bar{y}_3} \Omega(y_3^f) \tag{47}$$

The main result of the paper summarizes this discussion.

Theorem 1: (Main result) Under Assumptions 1, 2, 3 and 4, Problem 1 has a solution if and only if $y^0 \in \mathcal{F}^{sol}$. When $y^0 \in \mathcal{F}^{sol}$, the optimal thrust program is min-max, where one arc may be absent.

Remark 1: Without Assumption 4, max-min-max programs (where one or two arcs may be absent) are optimal.

V. NUMERICAL RESULTS

Let us consider the following (normalized) parameters

$$\kappa = 0.00285\,\mathrm{s}^{-1}, \quad r = 4.0, \quad \underline{y}_3 = 458.3\,\mathrm{s}, \quad \bar{y}_3 = 520.3\,\mathrm{s}.$$

In this example, the engine can be used at 60-100% of its maximum flowrate. Also, κ is taken close to the values of actual reusable launcher engines [21], such as the Merlin (Falcon 9) or the BE-4 (New Glenn). We consider a pressure model describing Earth's atmosphere from tabulated values, satisfying Assumption 1, s.t. $\pi(0) = 6.2 \times 10^{-1}$. Assumption 2 and 3 are satisfied since

$$\underline{a_{cc}} = 2.90 \times 10^{-3} > 0 \text{ and } \bar{b}/\sqrt{\underline{a}} = 3.37 \times 10^{-1} < 1.$$

$\mathcal{F}^{sol}$ is pictured in Figure 3 for these values. Assumption 4 is then checked numerically, by computing R_1 and $\frac{dy_3^f}{dt_1}(0)$ on a high density mesh covering $\mathcal{F}^{sol}$. The evaluation of (45) only requires to integrate ODEs, namely (4), (39) and (40), over fixed time intervals. Thus, it is vastly beneficial to use (45) instead of finite differences to check Assumption 4 in reasonable time.

To illustrate the optimality of the min-max structure, let us consider an example where three trajectories start from $y_1^0 = 1.25\,\mathrm{s}$, $y_2^0 = $ -6.96 $\times 10^{-2}$ and $y_3^0 = 441.2\,\mathrm{s}$, as presented in Figure 4. The trajectory with the min-max structure has the greatest final mass. The other two trajectories have respectively a 2.2% and 5.7% lower

Authorized licensed use limited to: ECOLE DES MINES PARIS. Downloaded on February 10,2022 at 09:24:16 UTC from IEEE Xplore. Restrictions apply.

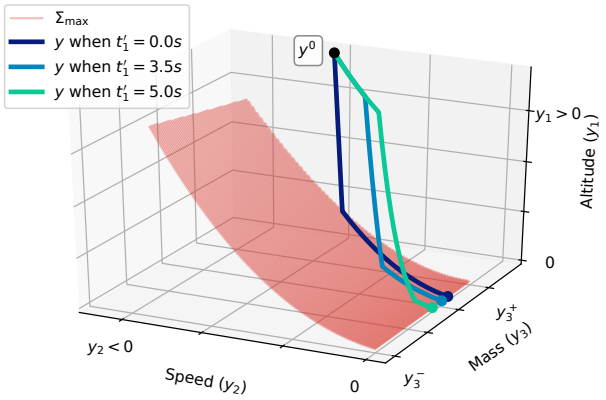

Fig. 4. Three max-min-max trajectories, with varying first time of switch t_1'. Maximum final mass is obtained for $t_1' = 0$, ie for a min-max thrust program.

final mass. Note that the associated time-of-flights t_f are respectively 25.6 s, 31.7 s and 41.1 s.

VI. CONCLUSION AND FUTURE WORKS

The theoretical results presented in this paper formulate assumptions under which the fuel-optimal atmospheric vertical powered landing has a very simple min-max structure. These assumptions take the form of an inequality that can be estimated numerically.

Some more subtle effects of the atmosphere could, in principle, be accounted for under the form of more advanced models. To improve representativeness, drag effects in the wake of the thrust flame could be additionally modeled. In view of applications, the resulting open-loop strategy has to be complemented by a closed-loop strategy to cope with model uncertainties and un-modeled disturbances. Another reason to develop a closed-loop strategy is that, as many bang-bang laws, the min-max solution is not robust. As-is, any actuator delay would necessarily lead to a crash. One solution is to use more conservative constraints $(\underline{Q}, \overline{Q})$, and exploit the remaining leeway with predictors, feedforward and feedback actions. This will be the subject of our future work.

VII. APPENDIX

A function $F : I \times \mathcal{X} \subset \mathbb{R} \times \mathbb{R}^n \to \mathbb{R}^n$ is said to be *quasi-monotone increasing* if, for every pair (t, x) and (t, v) in $I \times \mathcal{X}$ and every $i = 1, \ldots, n$, one gets $F_i(t, x) \geq F_i(t, v)$ whenever $x_i = v_i$ and $x \geq v$.

Lemma 5: (adapted from [22, IX.2.6]) Let F be a continuously-differentiable, quasi-monotone increasing function and $x : [t_0, \tau) \to \mathbb{R}^n$ the maximal solution of $\dot{x}(t) = F(t, x(t))$ through some point $(t_0, x^0) \in I \times \mathcal{X}$. Assume $v : [t_0, \tau') \to \mathbb{R}^n$, $\tau' \leq \tau$ is a differentiable function s.t. $(t, v(t)) \in I \times \mathcal{X}$ and (i) $v(t_0) \leq x^0$, (ii) $\dot{v}(t) \leq F(t, v(t)), \quad \forall t \in (t_0, \tau')$. Then, $v(t) \leq x(t)$ for any t in $[t_0, \tau')$. If $\leq$ is replaced by $\geq$ in (i) and (ii), then $v(t) \geq x(t)$ for any t in $[t_0, \tau')$.

REFERENCES

[1] J. Meditch, "On the problem of optimal thrust programming for a lunar soft landing," *IEEE Transactions on Automatic Control*, vol. 9, pp. 477–484, Oct. 1964.

[2] Y.-Y. Shi and M. Eckstein, "An exact solution for optimum controlled soft lunar landing," *Astronautica Acta*, vol. 16, pp. 9–18, 1971.

[3] L. Blackmore, B. Açıkmeşe, and J. M. Carson, "Lossless convexification of control constraints for a class of nonlinear optimal control problems," *Systems & Control Letters*, vol. 61, pp. 863–870, Aug. 2012.

[4] M. Szmuk and B. Acikmese, "Successive Convexification for 6-DoF Mars Rocket Powered Landing with Free-Final-Time," in *2018 AIAA Guidance, Navigation, and Control Conference*, American Institute of Aeronautics and Astronautics, 2018.

[5] U. Lee and M. Mesbahi, "Constrained Autonomous Precision Landing via Dual Quaternions and Model Predictive Control," *Journal of Guidance, Control, and Dynamics*, vol. 40, no. 2, pp. 292–308, 2017.

[6] I. M. Ross and M. Karpenko, "A review of pseudospectral optimal control: From theory to flight," *Annual Reviews in Control*, vol. 36, pp. 182–197, Dec. 2012.

[7] E. Brendel, B. Hérissé, and E. Bourgeois, "Optimal guidance for toss back concepts of Reusable Launch Vehicles," in *EUCASS 2019*, July 2019.

[8] Y. Ulybyshev, "Optimization of three-dimensional lunar landing trajectories and accessible area computation," in *AIAA Scitech 2019 Forum*, p. 0668, 2019.

[9] R. H. Goddard, *A Method Of Reaching Extreme Altitudes*. Baltimore, MD. U.S.A.: Smithsonian Institution, 1920. Publication 2540.

[10] B. Bonnard, L. Faubourg, and E. Trélat, "Optimal control of the atmospheric arc of a space shuttle and numerical simulations with multiple-shooting method," *Mathematical Models and Methods in Applied Sciences*, vol. 15, pp. 109–140, Jan. 2005.

[11] C. D'Souza, "An optimal guidance law for planetary landing," in *Guidance, Navigation, and Control Conference*, p. 3709, 1997.

[12] T. P. Reynolds and M. Mesbahi, "Optimal Planar Powered Descent with Independent Thrust and Torque," *Journal of Guidance, Control, and Dynamics*, vol. 43, pp. 1225–1231, July 2020.

[13] K. Graichen and N. Petit, "Solving the Goddard problem with thrust and dynamic pressure constraints using saturation functions," *IFAC Proceedings Volumes*, vol. 41, no. 2, pp. 14301–14306, 2008.

[14] E. Trélat, "Optimal control and applications to aerospace: some results and challenges," *Journal of Optimization Theory and Applications*, vol. 154, no. 3, pp. 713–758, 2012.

[15] H. Schättler and U. Ledzewicz, *Geometric Optimal Control: Theory, Methods and Examples*, vol. 38. New York: Springer Science & Business Media, 2012.

[16] F. W. Leslie and C. G. Justus, *The NASA Marshall Space Flight Center Earth Global Reference Atmospheric Model, 2010 Version*. National Aeronautics and Space Administration, Marshall Space Flight Center, June 2011.

[17] A. E. Bryson, *Applied optimal control: optimization, estimation and control*. CRC Press, 1975.

[18] R. Vinter, *Optimal control*. Springer Science & Business Media, 2010.

[19] R. Montgomery, "Abnormal minimizers," *Siam Journal on control and optimization*, vol. 32, no. 6, pp. 1605–1620, 1994.

[20] A. A. Agrachev and A. V. Sarychev, "On Abnormal Extremals for Lagrange Variational Problems," *Journal of Mathematical Systems Estimation and Control*, vol. 8, no. 1, pp. 87–118, 1995.

[21] A.-I. Onel, O.-I. Popescu, A.-M. Neculaescu, T.-P. Afilipoae, and T.-V. Chelaru, "Liquid rocket engine performance assessment in the context of small launcher optimisation," *INCAS Bulletin*, vol. 11, no. 3, pp. 135–145, 2019.

[22] N. Rouche, P. Habets, and M. Laloy, *Stability Theory by Liapunov's Direct Method*, vol. 4 of *Applied Mathematical Sciences*. Springer, 1977.

Authorized licensed use limited to: ECOLE DES MINES PARIS. Downloaded on February 10,2022 at 09:24:16 UTC from IEEE Xplore. Restrictions apply.